

Supporting Information

A high-performance composite fiber with organohydrogel sheath for electrocardiogram monitoring

Boya Chang,^a Jiabei Luo,^a Juan Liu,^b Bin Zhang,^a Ming Zhu,^a kerui Li,^a Yaogang Li,^c Qinghong Zhang,^c Guoying Shi,^{*d} and Chengyi Hou^{*a}

a. State Key Laboratory for Modification of Chemical Fibers and Polymer Materials, College of Materials Science and Engineering, Donghua University, Shanghai 201620, P. R. China.

b. Shanghai Academy of Spaceflight Technology (SAST), Shanghai, 201109, P. R. China.

c. Engineering Research Center of Advanced Glasses Manufacturing Technology, Ministry of Education, College of Materials Science and Engineering, Donghua University, Shanghai 201620, P. R. China.

d. College of Chemistry, Chemical Engineering and Biotechnology, Donghua University, Shanghai, 201620, PR China.

* Corresponding author:

E-mail address: shigy@dhu.edu.cn; hcy@dhu.edu.cn (Chengyi Hou)

This file includes:

Figure S1 to S13

Movie

S1

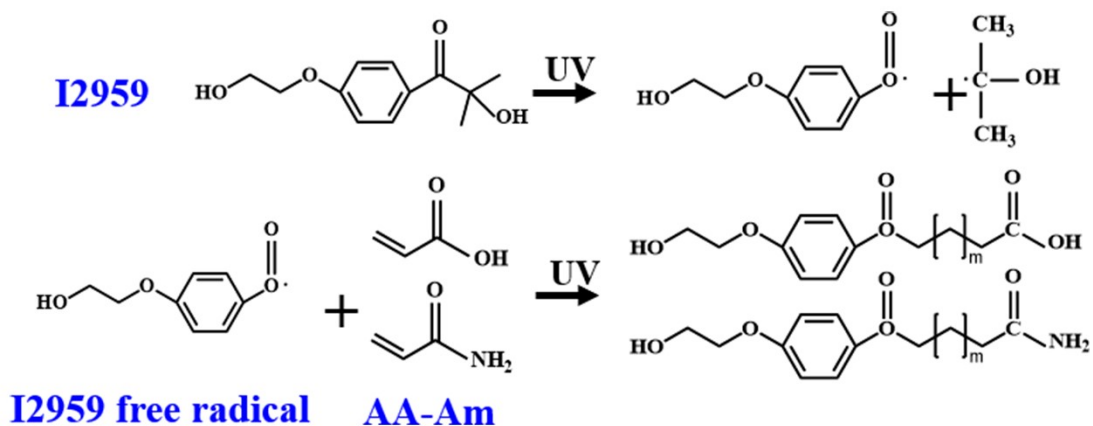


Figure S1. Photoinitiator I2959 produces free radicals to participate in polymerization.

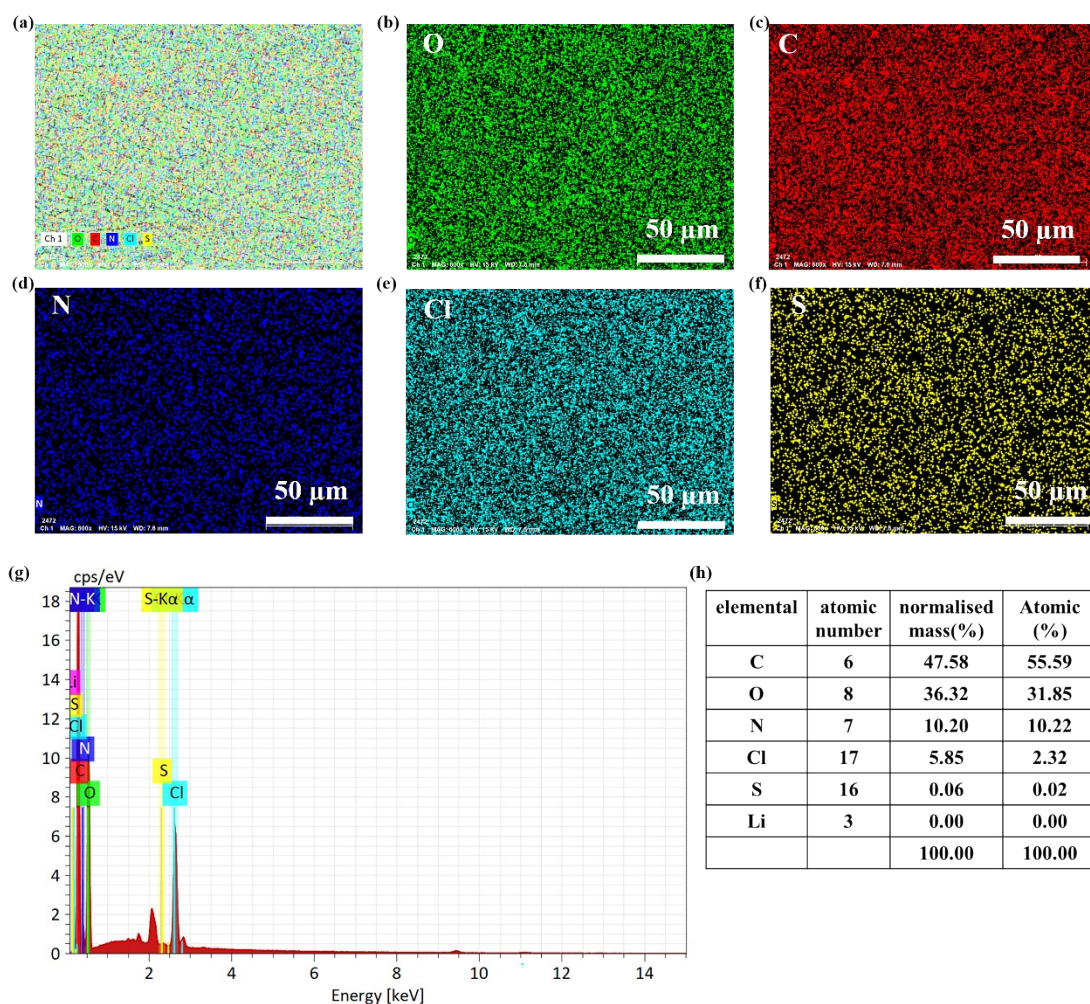


Figure S2. Energy dispersive spectroscopy tests of elemental oxygen, carbon, nitrogen, chlorine, and sulfur in organohydrogels. (a~f) Elemental distribution spectra. (g) Elemental distribution line profiles. (h) Relative content of each element in the organohydrogel.

The test results are as follows:

To ascertain the homogeneous distribution of lithium in the organohydrogel, we conducted energy dispersive spectroscopy (EDS) tests. In the organohydrogel preparation, lithium chloride gradually dissociates into lithium and chloride ions. These ions are mobile in solution, and their distribution follows similar diffusion and exchange mechanisms. Chlorine, with a high characteristic energy (~ 2.62 keV), is easily detected by EDS. Therefore, by measuring the distribution of elemental chlorine, the distribution of elemental lithium in the hydrogel can be inferred. The test results demonstrate that the distribution of chloride ions is homogeneous.

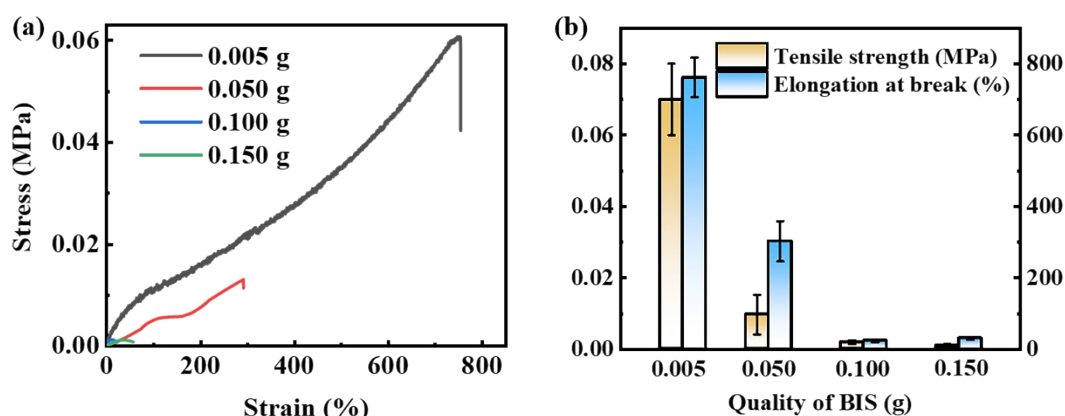


Figure S3. Mechanical properties of organohydrogels with different BIS qualities tested.

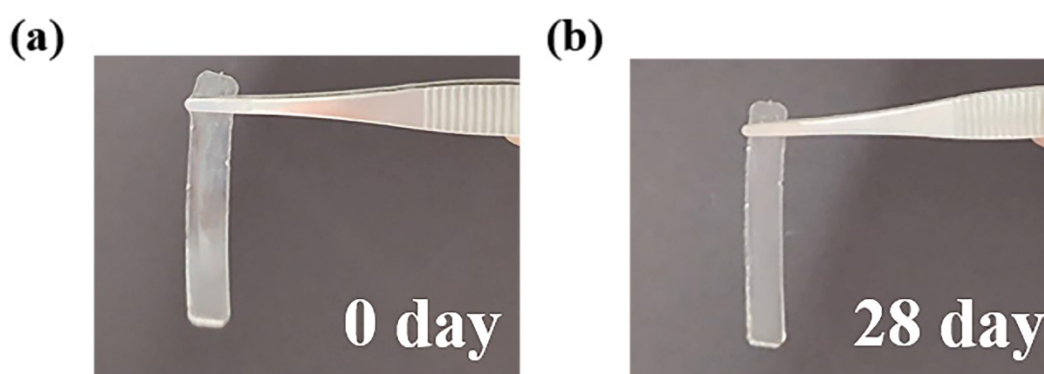


Figure S4. Physical comparison of the ionic gel before and after 28 days of placement.

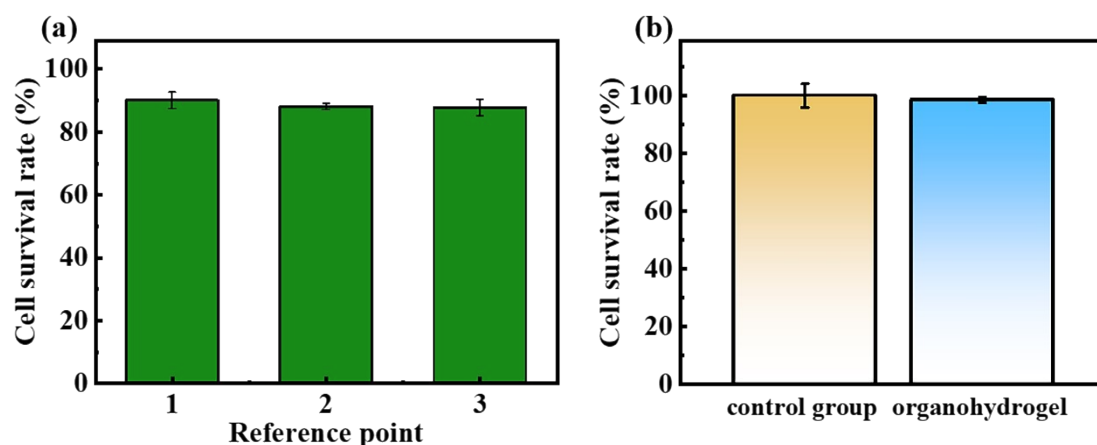


Figure S5. Biocompatibility testing of organohydrogels. (a) Cell viability test of organohydrogel samples after 24 hours of placement. (The organohydrogel sample was placed in a petri dish for 24 hours and three locations in the dish were selected for cell staining and labelled 1, 2 and 3) (b) Assessment of cell viability following the 72 hours placement of the organohydrogel. (The yellow bars represent the blank control group, while the blue bars represent the organic hydrogel, which exhibited a 98% cell survival rate.)

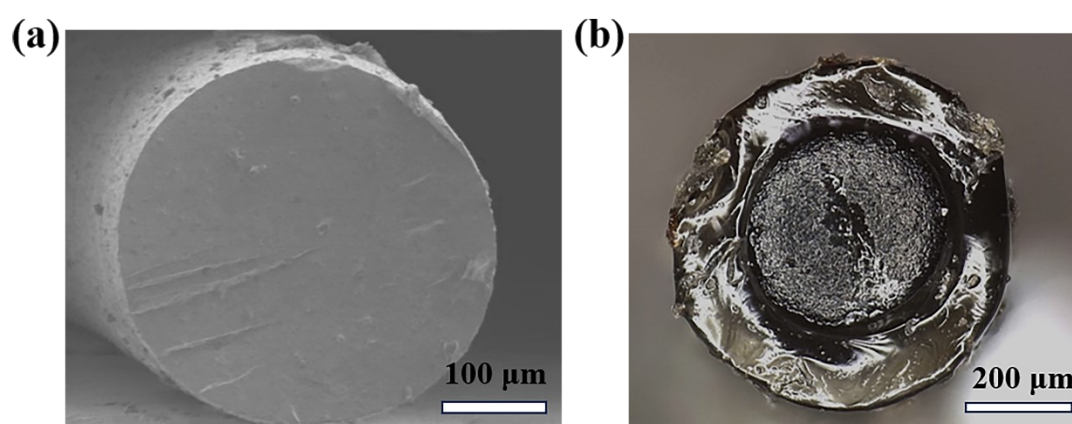


Figure S6. Sectional morphology of SCP and CF fibers. (a) Scanning electron microscope image of SCP fibers. (b) super field image of CF fibers.



Figure S7. The condition of the organohydrogel on the skin before and after 8 hours showed no signs of redness, swelling, or allergic reactions.

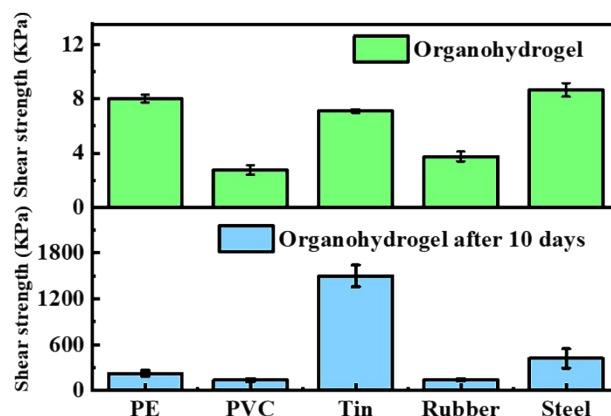


Figure S8. The shear strength and interfacial toughness of SF organohydrogel on different substrates after storage in 40% relative humidity at 20 °C for 10 days

The test results are as follows:

A series of tests were conducted to assess the shear strength of the organohydrogel after being exposed to conditions of 40% humidity and 20 °C for 10 days. The results indicated a significant increase in shear strength for PE, PVC, tin, rubber, and steel, with enhancements of 2712%, 4809%, 21026%, 3633%, and 4755%, respectively. It is hypothesized that the reduction in water content within the organohydrogel causes the polymer network to contract, potentially increasing surface chain density and enhancing adhesive properties (Polymer, 2022, 246, 124730).

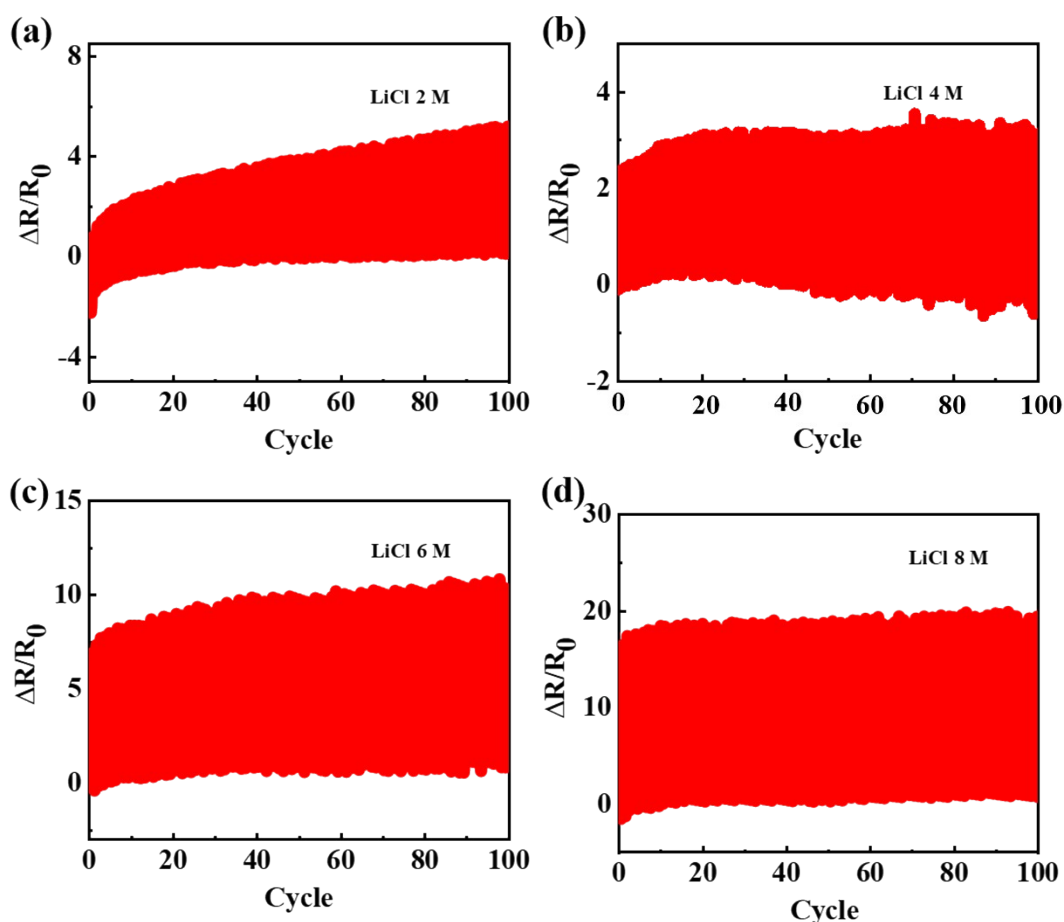


Figure S9. Electrical tensile cyclic stability test of organohydrogels with different LiCl contents.

The test results are as follows:

Figure S9 illustrates the cyclic stability of resistivity stretching under 30% strain for organohydrogels with varying lithium chloride concentrations. At low lithium chloride concentrations, there is a slight fluctuation in the resistance change of the gel electrode, but the overall change is not significant. However, at higher lithium chloride concentrations, while the change in resistivity is smaller, the resistance change during stretching becomes more pronounced. This phenomenon may be attributed to the oversaturation of salt ions in the precursor solution and irregular particle accumulation, which affect the interaction forces between molecular chains in the conductive network, resulting in irregular changes in resistivity during stretching.

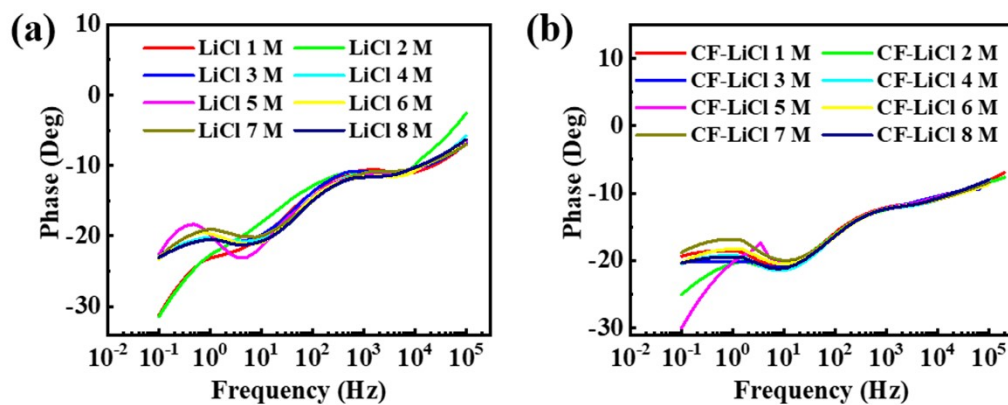


Figure S10. Angle diagram of ion-gel fiber electrode and ion-gel composite skin core fiber electrode with different LiCl concentration.

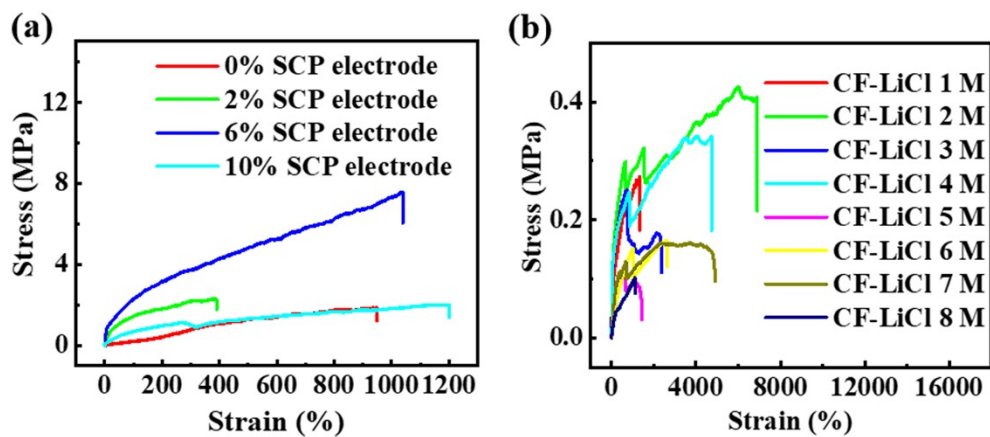


Figure S11. Stress-strain test diagram of SCP dry electrode and CF electrode.

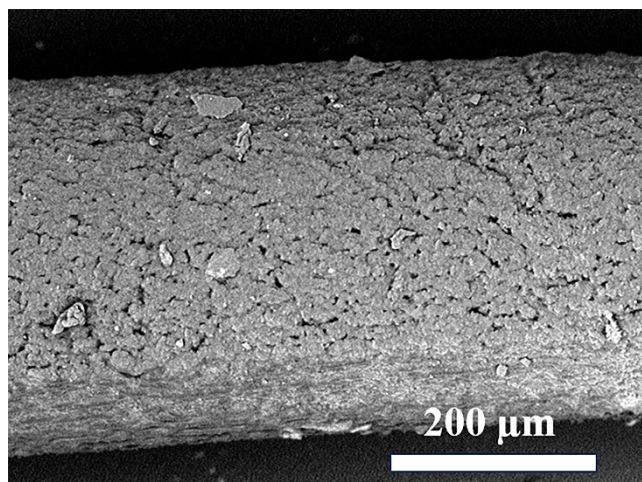


Figure S12. Scanning electron microscope image of the surface of the SCP fiber dry electrode.

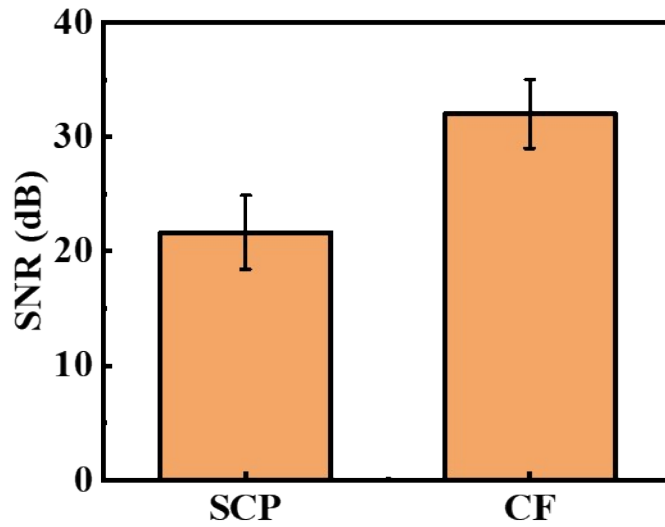


Figure S13. Electrocardiographic testing of SCP dry electrodes and composite CF electrodes in the resting state. (The average signal-to-noise ratio was approximately 21 μ V for the SCP dry electrode and 32 μ V for the CF electrode.)

Supplementary Video

Video S1 ECG signal acquisition with CF electrodes and dry SCP fiber electrodes.